Enhancement of the capability of a three-dimensional particle tracking system by integration of an electrically focus-tunable lens

Project Report

Presented in Partial Fulfillment of the Requirements for the Degree Master of Science in the Graduate School of The Ohio State University

By

Tushar Agarwal

Graduate Program in Mechanical Engineering

The Ohio State University

2017

Master's Examination Committee:

Professor Chia-Hsiang Menq, Advisor

Professor Krishnaswamy Srinivasan

Abstract

The objective of this project is to design a control system for an electrically focus tunable lens, such that the net resultant focal plane of the microscope optical system tracks an axially moving microscopic particle. In the past, it has been achieved by using lenses mounted on mechanical actuators. Such systems have a few drawbacks of limited movement range, slower response times and vibrations in the system. A discrete time PI controller is designed for the electrically focus tunable lens which achieves the tracking objective. The problem of lack of direct state feedback information is tackled through state estimation. A combination of three mathematical models and image processing achieves this task of state estimation. The control system is then successfully simulated and experimentally tested.

Acknowledgements

I would like to thank my advisor, Professor Chia-Hsiang Menq. During my time at Ohio State, he has afforded me many valuable opportunities that have greatly contributed to my success in graduate school. His guidance towards my research project as well as in the classroom, has greatly improved my research and engineering skillset. I thank my colleagues in the Precision Measurement and Control Laboratory, especially Dr. Cheng, Yanhai and Ta-Min, for their assistance in research and otherwise; they made my research experience in the lab memorable. I also thank Mr. Kevin Wolf for his assistance in manufacturing of an essential experimental component.

I am extremely grateful to all the friends at the university and in particular, Ritika, who provided essential help in programming part of the project.

I am indebted to the Department of Mechanical and Aerospace engineering for providing me financial support through a Graduate Teaching Associate appointment.

Finally, I would like to give a sincere thanks to my loving family. My parents have always nurtured my desire to learn and have continually encouraged me throughout my education despite of their circumstances back home. My brother has been immensely supportive of my entire graduate school endeavor. I am especially grateful for the understanding he showed as well as moral and financial support he provided throughout my studies at Ohio State.

Vita

May 2011.....Delhi Public School, Azad Nagar, Kanpur

2015 .....B.Tech., Mechanical Engineering, Indian Institute of Technology (I.S.M.) Dhanbad

2016 to present .....Graduate Teaching Associate, Department of Mechanical Engineering, The Ohio State University

Fields of Study

Major Field: Mechanical Engineering

Table of Contents

Table of Contents

Introduction

Since their invention in the 16th century Europe, microscopes provide the most common means of observing biological phenomenon at the microscopic level. However, many biological phenomena and corresponding particles exhibit mobility in the direction not contained in the plane of the stage. This poses a problem in observing these phenomena as microscopes are designed to have a static focus which causes the biological particles to go out of focus and inhibits proper observation of the processes. In the past, a common solution to this problem has been a moving stage or lens which moves as the particles move along the z-axis. This approach has its disadvantages such as limited physical space for movement, slower response time compared to the movement speed of the particles and vibrations due to the movement.

This project aims at another approach of solving the problem of automatic focusing of moving biological particles. An electrically focus tunable lens is utilized Optotune's shape-changing lens is based on this principle and elastic polymer materials. The core element of the lens consists of a thin membrane that builds an interface between a liquid-filled chamber and air (Figure 1). A current-controlled electromagnetic or mechanical actuator pushes down on the liquid-filled lens container, forcing the lens liquid into the center of the lens and changing its shape. Controlling the electrically tunable lens (ETL) is hence, straightforward, requiring only a current controller or lens driver to supply the lens with a current.

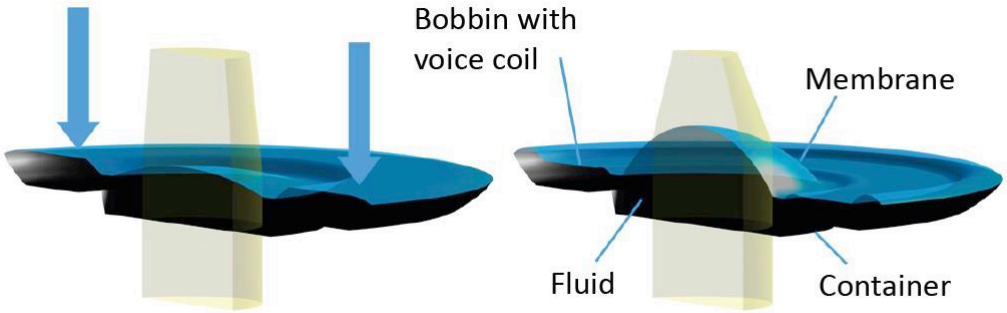

Figure 1: Scheme of the sealed lens container filled with an optical fluid and embedded in an EL-16-40-TC housing. [1]

In designs for auto-focusing systems, a significant trade-off exists between cost and complexity. Unlike deformable mirrors or spatial light modulators, most tunable lenses have only a single degree of freedom, namely the focal length. A microscope equipped with a single ETL in a remote-focusing path cannot perform the same sophisticated aberration corrections over the Z-tuning range as a true adaptive optics microscope. However, focusing with an ETL comes at a tiny fraction of the cost of a fully-fledged adaptive optics setup. Hence, this project is an effort to make better use of its capabilities. Using an ETL, a computer controlled auto-focusing system is designed based upon a basic PI controller and image processing.

The following notation is used here after:

Symbol	**Description (units, range)**
z_p	$z-axis\ \ position\ of\ the\ particle\ (\mu m, z_p \in [0, 20]\ )$
z_f	$z-axis\ \ position\ of\ the\ net\ resultant\ focal\ plane\ (\mu m)$
i	$current\ input\ to\ lens\ (mA, i \in [0, 292.84])$
I	$intensity\ of\ the\ image$
Δz	$difference\ between\ z-axis\ \ positions\ of\ the\ \ particle\ \&\ focal\ plane\ (\mu m)$
$\hat{q}$	$estimated\ value\ of\ any\ quantity\ "q"$

Control System Design

The primary challenge in making this control system is the lack of direct feedback of z-axis position of focal plane of the microscopic system. The image through a camera is the only feedback information available. Image processing and modeling is required to predict the error between the particle and focal plane positions, i.e.:

$$error = \Delta z = z_p - z_f$$

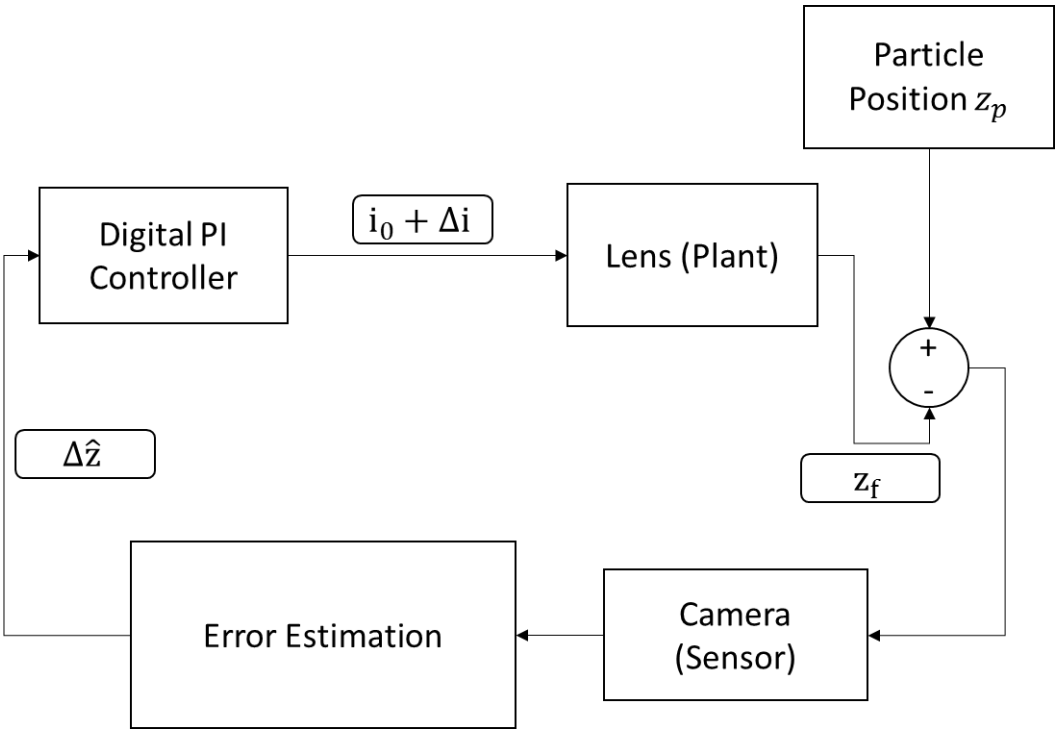

Figure 2: System Block Diagram

Experimental Setup

The measurement system and associated experimental apparatus are set up on a modified inverted microscope (Nikon TE2000-U) equipped with a 60× water immersion objective lens (Plan Apochromat 60× WI). Considering the 60× magnification of the objective lens, a 1.5× intermediate magnification, and a 0.6×

magnification of the C-mount adaptor, the total optical magnification is 54× in the system.

An electrically tunable Optotune lens (EL-16-40-TC) is used with a power range of -2 to +3 diopters for the nominal control current -250 to +250 mA. This control current is provided by Optotune Electrical Lens Driver 4 which in turn is connected to the computer via. a USB cable and accepts control commands using serial communication. However, to incorporate this lens in the inverted microscope setup, a suitable adapter was needed. This adapter was designed and 3-D printed in the Student Shop of Department of Mechanical and Aerospace Engineering at The Ohio State University. Figure 3 shows the adapter, containing the ETL and fitted in the microscopic setup.

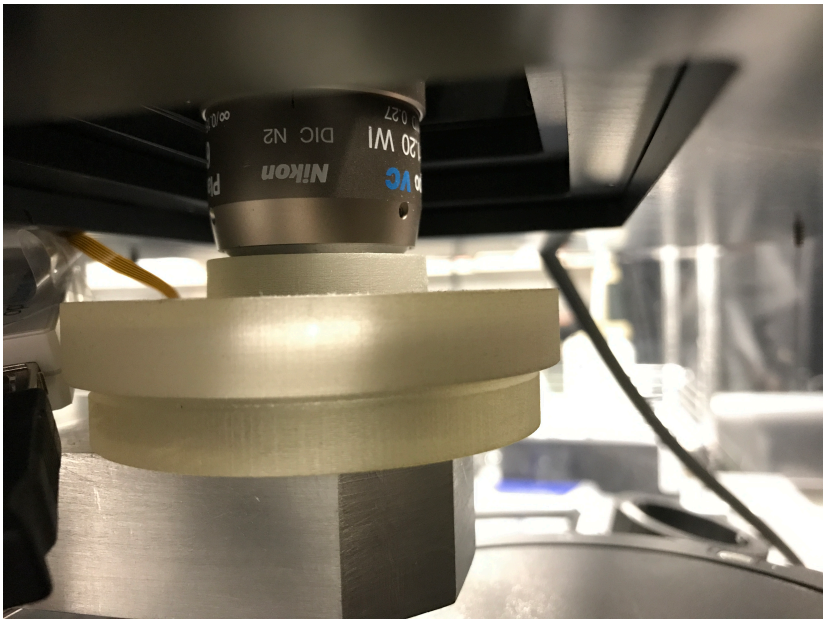

Figure 3: Custom made adapter containing ETL

A CCD camera (Photometric CoolSNAP-EZ) is connected to the computer (HP workstation CQ5210F, AMD Athlon II X2 2.70 GHz CPU, 3 GB RAM) through an CoolSNAP IEEE-1394 cable and a CoolSNAP IEEE-1394 interface card that has been installed in the host computer. The communication rate can reach 10 frames per second for the 12 bit 1392 x 1040 size images. This means the least possible sample time of this discrete-time control system can be $T_s = 0.1\ s$, i.e., limited by the FPS of the camera. Decreasing the image size can proportionally increase the

sampling rate. The pixel size is 6.45 × 6.45 μm^2. Therefore, at the sampling plane, the spatial sampling width is $\frac{6.45\ \mu m}{54} = 119.44\ nm$.

A 3-axis piezo stage (Physik Instrumente, E-710) is assembled on top of the microscope's manual planar stage to provide fine 3D motion. It is connected to the computer through serial communication. The piezo stage provides subnanometer precision motions in all three translational directions and its motion range is $100\ \times\ 100\ \times\ 20\ \mu m^3$. It is employed in the automated calibration process and also used to provide reference trajectories for verifying the tracking algorithm.

The particle position, z_p, is controlled by the piezo-stage for calibration and experimental purposes. All the devices are controlled through MATLAB R2014b running on the computer.

Metrics for Modeling

Finding the appropriate metrics for modeling and estimation of Δz from the image, is one of the most critical task of this project. Several options, as mentioned in [2], are explored and finally two functions are found suitable for this application.

A function F is evaluated from the image matrix which is a metric of sharpness of the image based on its normalized variance.

$$F = \frac{1}{H.W.\mu}\sum_{y=1}^{H}\sum_{x=1}^{W}(I(x,y)-\mu)^2$$

Where H is no. of rows in image intensity matrix, W is no. of columns in image intensity matrix and μ is the average of the image intensity matrix.

This function has a distinct maximum when the image is in focus. The validity of this function is tested by performing several experimental trials where Δz is varied from -2 to 2 μm. by varying z_p and keeping z_f constant. Before each trial, a different z_p is chosen and particle is manually brought in focus such that $z_f = z_p$.

The z-axis positions where z_f is made equal to z_p are referred to as mean positions henceforth. The results are shown in Figure 4.

Clearly, the curve varies a little for every mean position but all curves have a distinct maximum at $\Delta z = 0$, thus, verifying the claims.

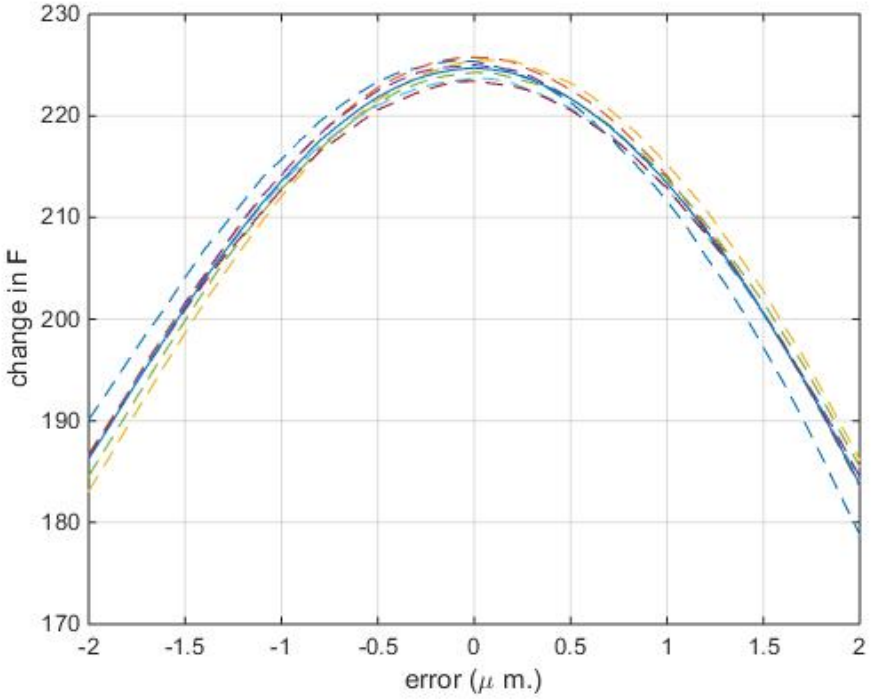

Figure 4

Another function, R, is evaluated during experimental calibration which is the root mean squared value of all the image intensities in the image matrix.

$$R = \sqrt{\frac{1}{H.W}\sum_{y=1}^{H}\sum_{x=1}^{W}\big(I(x,y)\big)^2}$$

This function is proportional to the image power and it is intuitive that it should continuously increase as the particle moves closer to the light source, i.e., upwards in an inverted microscope.

Calibration of Models

A quasi-static calibration is done for a range of $\pm 0.4\ \mu m$ starting from 15 different equally spaced initial mean positions from $1\ \mu m\ to\ 15\ \mu m$.

At first, the image is brought in focus at every discrete step of the stage by using a golden section search for maximum value of sharpness metric F. This accomplishes the task of making $z_f = z_p$ where z_p is a known value of that mean position during calibration. The values of current input, i, to the lens and function R at each mean position (denoted as R_c) are evaluated, and plotted against the individual mean positions z_f. The results are shown in figures 4 and 5.

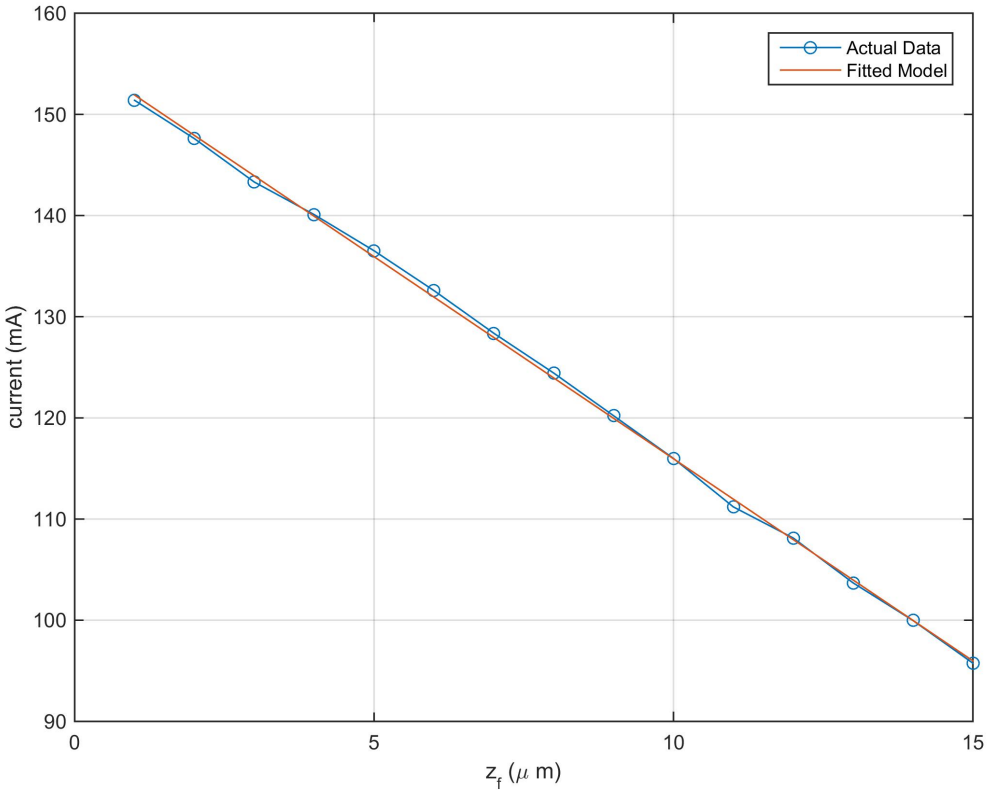

Figure 5

A linear model is fitted to the experimental values of $i\ vs.\ z_f$ shown by the blue curve in figure 5. The fitted model is shown as a red curve in the same figure. The general equation of this curve is of the form: -

$$i = a_1 z_f + a_0$$

(1)

A quadratic model is fitted to the experimental values of $R_c\ vs. z_f$ shown by the blue curve in figure 6. The fitted model is shown as a red curve in the same figure. The general equation of this curve is of the form: -

$$R_c = b_2 z_f^2 + b_1 z_f + b_0$$

(2)

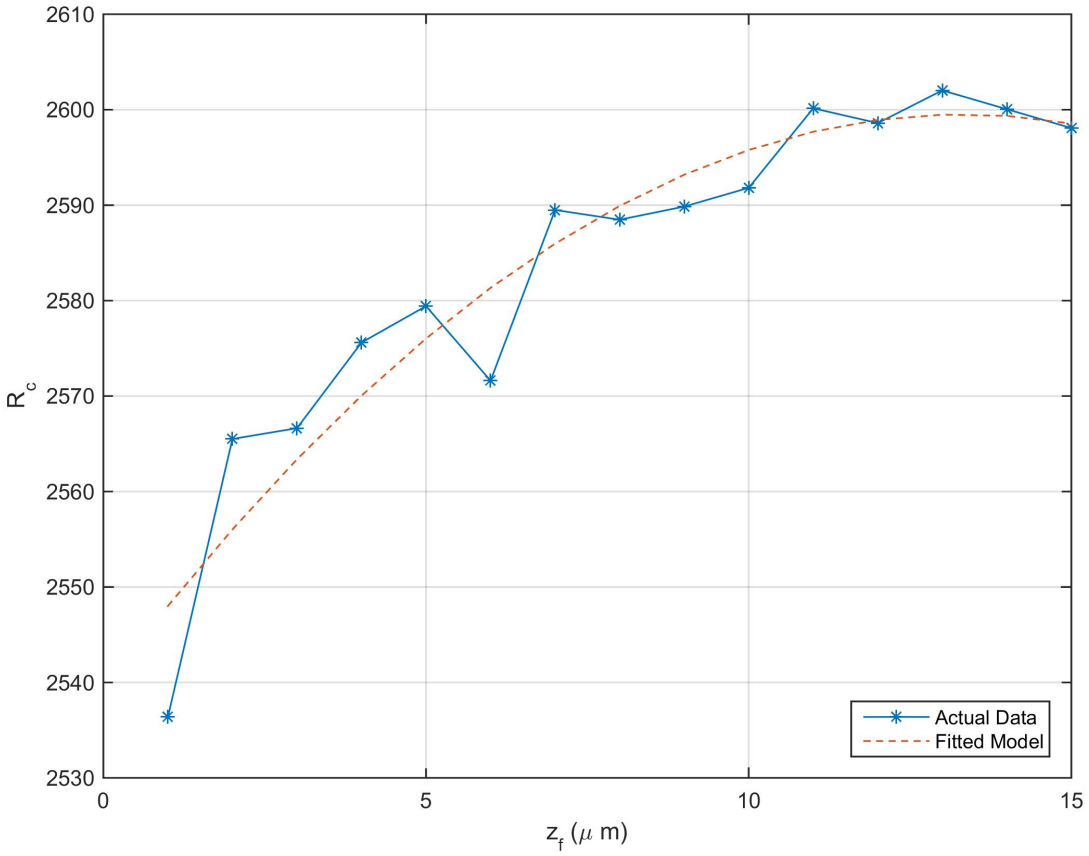

Figure 6

The deviation of value of function R from its mean position value is expressed as

$$\Delta R = R - R_c.$$

The results of $\Delta R\ vs.\ \Delta z$ are shown in figure 7. Each individual curve belongs to each of the 15 mean positions during calibration. Clearly, the curve varies a little for every mean position but all curves have an approximate linear trend. The variation in slopes of these curves is shown by plotting each slope vs. the corresponding z_f value. This is shown in figure 8.

Figure 7 also shows an averaged straight line curve for all these curves. The equation of this line is of the form: -

$$\Delta\hat{z} = c_1 \Delta R \tag{3}$$

This mean curve is used further for error estimation in tracking control.

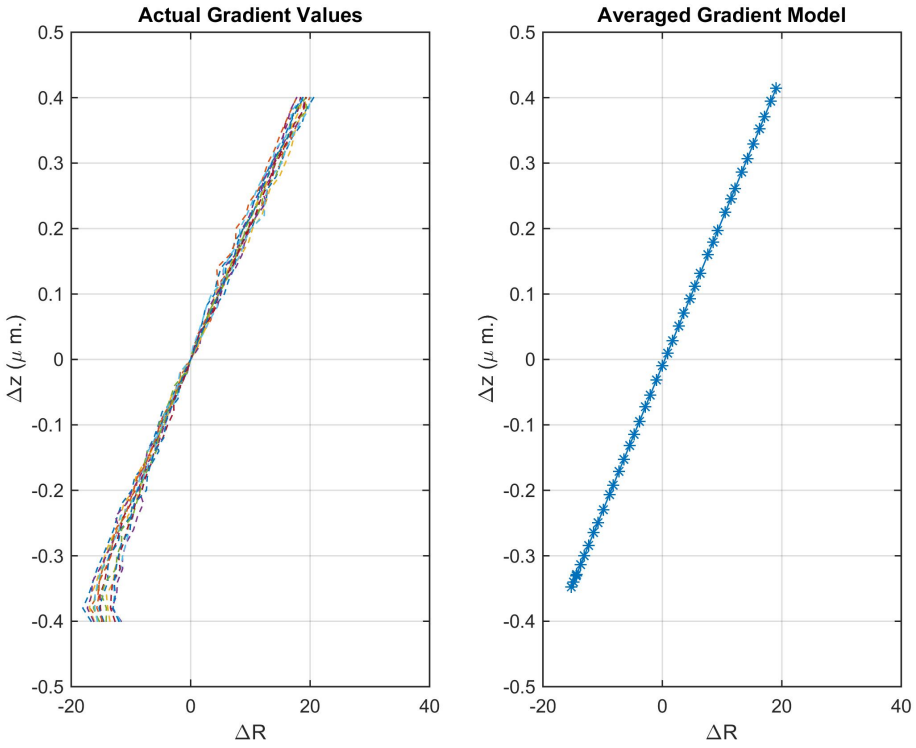

Figure 7

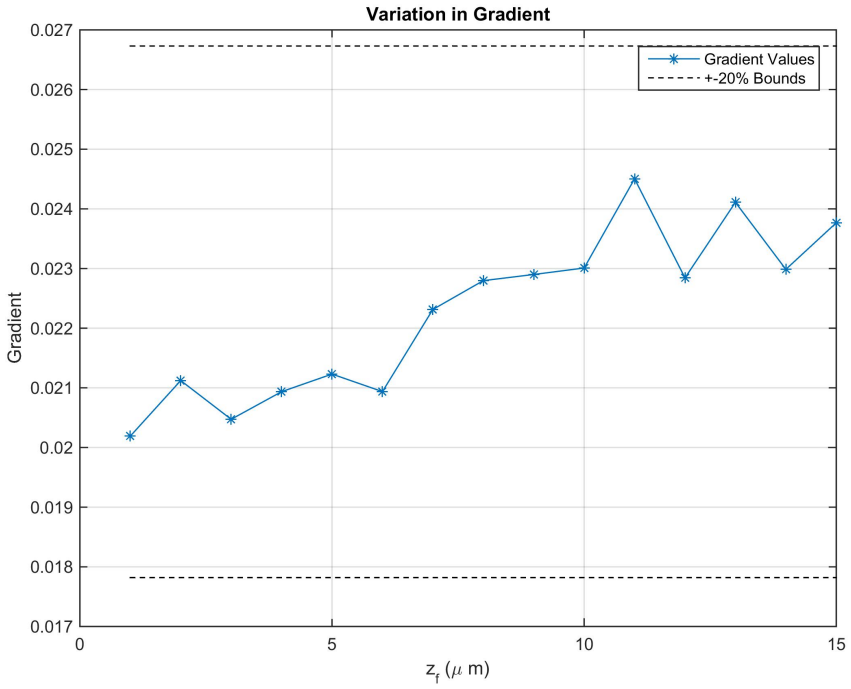

Figure 8

Tracking Algorithm

Lateral Motion Estimation

The lateral motion of a circular particle can be directly estimated from the acquired two-dimensional (2D) images using the centroid method. The centroid method is a robust, accurate, and fast technique that is widely accepted. The underlying assumption of the method is that the image is circularly symmetric and that the center of the bead is coincident with the centroid of the image.

In order to decrease estimation errors caused by nonuniform background noise, image preprocessing is often applied to eliminate or significantly reduce the effects of background noise. In this project, before calculating any metric from the image, a small region of interest (R.O.I) is extracted from the image obtained from the camera. For this, the image matrix is first normalized to values between 0 and 1. Then, the boundary of the particle in the image is located using thresholding at value of 0.8. The bwboundaries MATLAB function, used for this task, implements

the Moore-Neighbor tracing algorithm modified by Jacob's stopping criteria. This function is based on the boundaries function presented in the Appendix C of [3].

The x & y co-ordinates of the particle at any time instant can be estimated using the centroid of the region (or pixels) inside the estimated particle boundary. The coordinate of the centroid (x_c, y_c), and thus the position of the bead, in the camera coordinate system is calculated using the following equation:

$$(x_c, y_c) = \left(\frac{\sum_{x=1}^{W} \sum_{y=1}^{H} x \times I(x,y)}{\sum_{x=1}^{W} \sum_{y=1}^{H} I(x,y)}, \frac{\sum_{y=1}^{H} \sum_{x=1}^{W} y \times I(x,y)}{\sum_{x=1}^{W} \sum_{y=1}^{H} I(x,y)} \right)$$

The tracking in lateral direction, in this project, is limited to estimating lateral particle position in the image. However, if the particle moves out of the planar region of observation, there exists no mechanism in this experimental setup, to follow the particle in the lateral directions. This project focuses primarily on particle tracking in the axial direction, which is usually the more essential requirement in such situations.

Axial Motion Estimation

All the models are calibrated for axial motion estimation and tracking of the particle. The axial motion tracking algorithm is what follows.

Using $z_{f0} = 0$, and $i \; vs. \; z_f$ curve, the reference current bias, i_0, is estimated as: -

$$i_0 = a_1 z_{f0} + a_0 = a_0$$

The value of function R is calculated for the R.O.I. of the image and consequently, the Δz is estimated using the model as: -

$$\Delta \hat{z}(k) = c_1 \Delta R \Rightarrow \Delta \hat{z}(k) = c_1 \left(R - \hat{R}_c \right)$$

Where R_c is estimated using the model as: -

$$R_c = b_2 \hat{z}_f^2 + b_1 \hat{z}_f + b_0 = b_2 \left(\frac{(i - a_0)}{a_1} \right)^2 + b_1 \left(\frac{(i - a_0)}{a_1} \right) + b_0$$

A discrete time PI controller is used with the following equation: -

$$\frac{\Delta i(k)}{\Delta \hat{z}(k)} = K_p + K_I \frac{T_s}{2}\frac{z+1}{z-1}$$

$$\Rightarrow \Delta i(k) = \Delta i(k-1) + K_p[\Delta \hat{z}(k) - \Delta \hat{z}(k-1)] + K_I \frac{T}{2}[\Delta \hat{z}(k) - \Delta \hat{z}(k-1)]$$

Where K_p & K_I are proportional and integral gains respectively.

The input current to the lens is:

$$i(k) = i_0 + \Delta i(k)$$

The estimated values of z_f and z_p are then obtained as: -

$$\hat{z}_f(k) = \frac{i(k-1) - a_0}{a_1}$$

$$\hat{z}_p(k) = \hat{z}_f(k) + \Delta \hat{z}(k-1)$$

For the first time-step, it is assumed that the initial particle position, z_{p0} is known. Then

$$\Delta \hat{z}(0) = z_{p0} - z_{f0} = z_{p0}$$

$$\Delta i(0) = a_1 \Delta \hat{z}(0)$$

Design Decisions and Simulation Setup

At first, the digital control system is implemented in Simulink and tested for minimum possible sampling time, $T_s = 0.1\ s$. Then it was coded into MATLAB and and the computational time used by MATLAB in processing of one sample iteration of the tracking control loop commands was found. It turned out to be

0.14 s approximately. Hence, the simulation is run again for the actual sampling time, $T_s = 0.14\ s$

Another decision to be made is the gains of the PI controller, K_p & K_I. For this, the system is first reduced to a conventional discrete time closed loop system assuming that output z_f is directly available as feedback, as shown in figure 9.

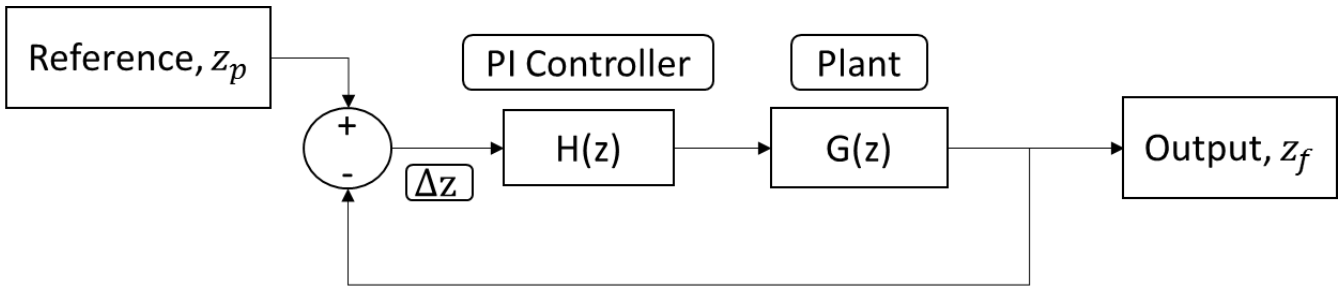

Figure 9

Where

$$H(z) = K_p + K_I \frac{T}{2}\frac{z+1}{z-1} = \frac{z\left(2K_p + K_I T_s\right) + \left(K_I T_s - 2K_p\right)}{2z-2}$$

&

$$G(z) = (1 - z^{-1})Z\left(\frac{G(s)}{s}\right)$$

The plant, i.e. the lens is assumed to have first order dynamics in continuous time, with a time constant $\tau = 0.015\ s$. The transfer function must also have a gain of $\frac{1}{a_1}$ to incorporate change of magnitude from current i to z_f. Hence,

$$G(s) = \frac{1}{a_1(\tau s + 1)}$$

For simulation purposes, a_1 is assumed to be -60 which is approximately the slope obtained from $i\ vs.\ z_f$ curve. Therefore,

$$G(z) = -\frac{1}{60(z - 8.843 \times 10^{-5})}$$

The closed loop transfer function will then be: -

$$\frac{z_f(z)}{z_p(z)} = \frac{H(z)G(z)}{1 + H(z)G(z)}$$

For pole placement, the characteristic equation of this closed loop system is-

$$z^2 - z\left[(1 + 8.843 \times 10^{-5}) + \frac{(2K_p + K_I T_s)}{120}\right] + \left[8.843 \times 10^{-5} + \frac{(2K_p - K_I T_s)}{120}\right] = 0$$

Let this 2nd order system be critically damped, i.e. damping ratio $\xi = 1$ and let the settling time be, $\tau_s = 0.1\ s$ $(= \frac{4}{\xi \omega_n}, \omega_n$ denotes natural frequency).

Therefore, both the poles in the s-plane will be at $s = -\xi\omega_n = -40$. Therefore, the poles in the z-plane will be at $z = e^{s \times Ts} = 0.0037$

Then

$$(1 + 8.843 \times 10^{-5}) + \frac{(2K_p + K_I T_s)}{120} = 2 * 0.0037 = 0.0074$$

$$8.843 \times 10^{-5} + \frac{(2K_p - K_I T_s)}{120} = 0.0037^2 = 1.3674 \times 10^{-5}$$

Solving these two equations for K_p & K_I yields

$$K_p = -29.7724 \ \ \& \ \ K_I = -425.4077$$

The Simulink implementation of the system is shown in figure 10. The models represented by Eqs. (1), (2) and (3) are calibrated on the real system and utilized in the simulation. The simulation also incorporates uniform random noise

introduced in calculation of R_c & R to make results more realistic and account for the measurement noise. All the Simulink blocks work on sampling time of $T_s = 0.14\ s$.

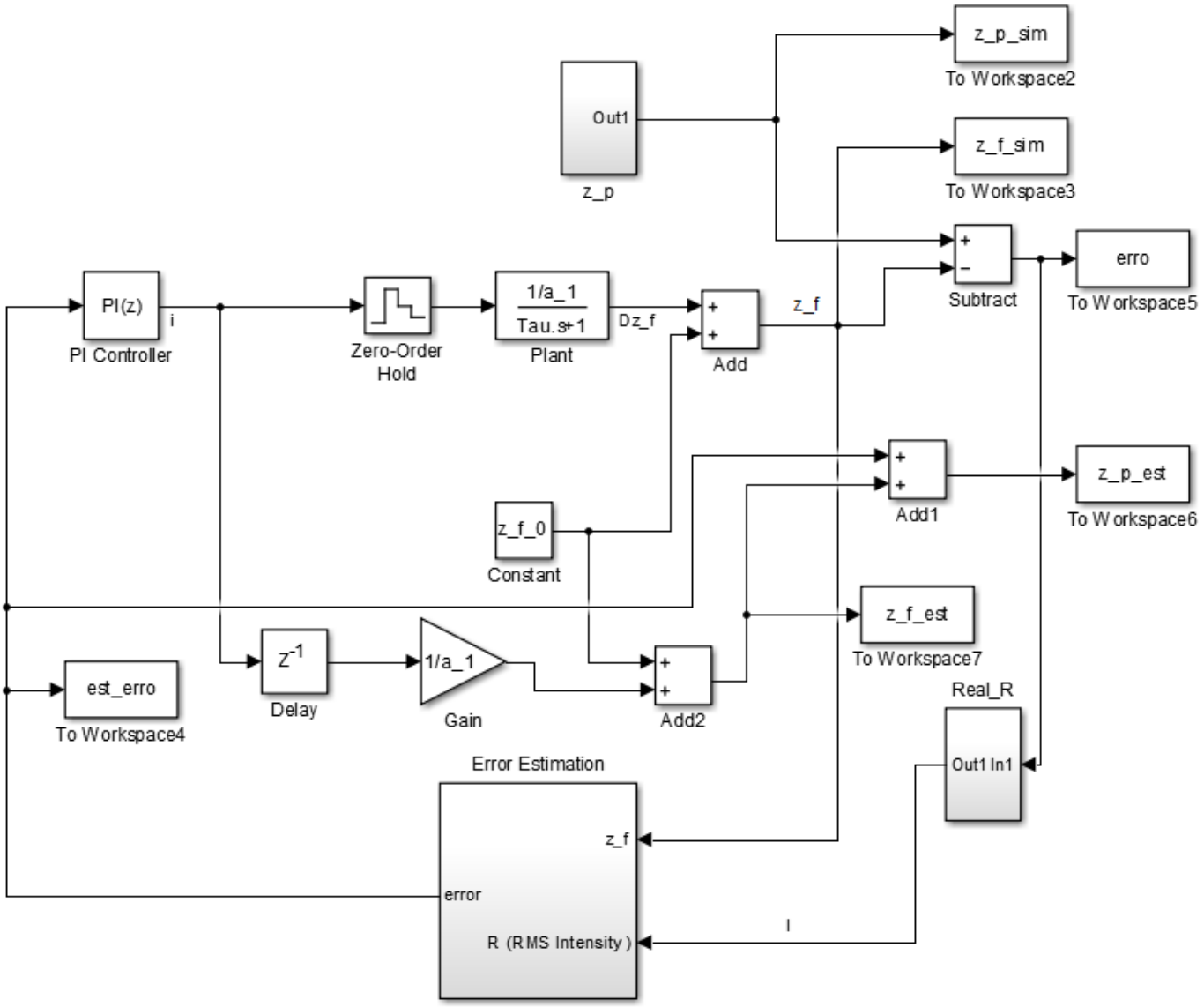

Figure 10

Results and Discussion

Simulation

The simulation is run for two types of input disturbances, z_p. First disturbance is a step input of 5 μm at time of 1.4 s. The results of this simulation are shown in figures 11 & 12. The actual and estimated values of error, shown in figures, are defined as $\Delta z = z_p - z_f$ & $\Delta \hat{z} = \hat{z}_p - \hat{z}_f$.

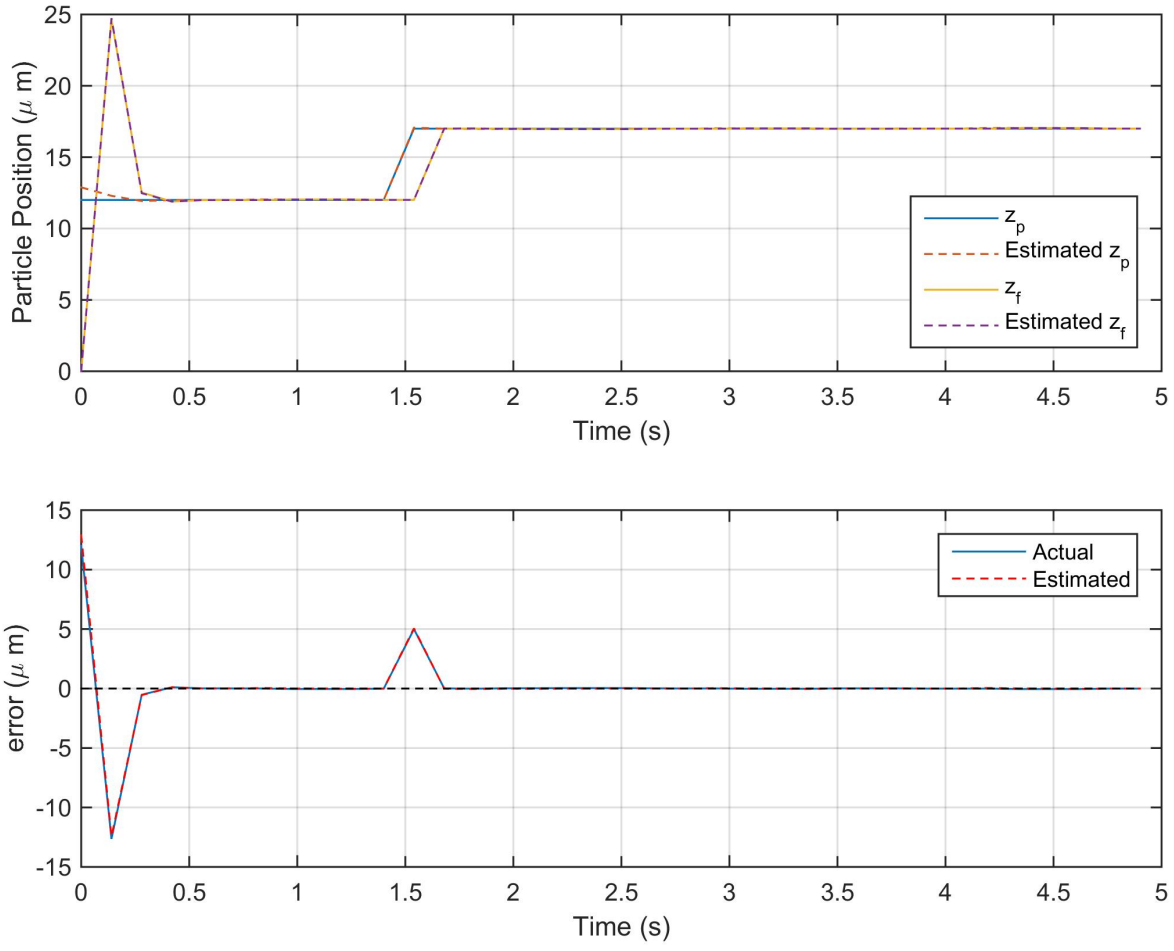

Figure 11

It can be seen in figure 11 that the system responds in 0.14 seconds, i.e., one sample time. This is obvious as the settling time is 0.1 s and for a discrete time system, the response will show up in the next time step from the disturbance which is 0.14 s apart.

Figure 12 shows that the actual and estimated values are close even in presence of noise.

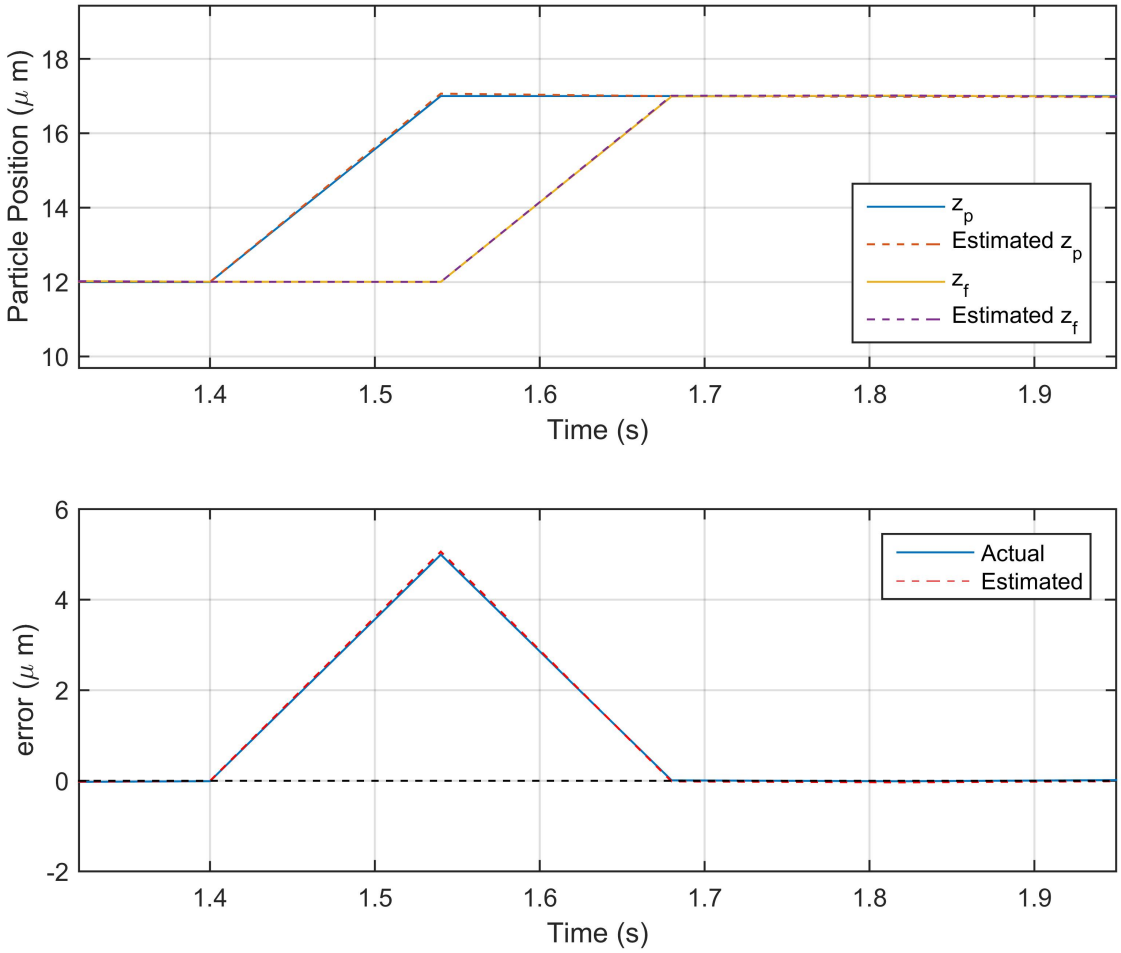

Figure 12: Figure 11 zoomed-in

The second disturbance is a triangular wave input of amplitude 2 μm and frequency 0.1 Hz. The results of this simulation are shown in figures 13 & 14.

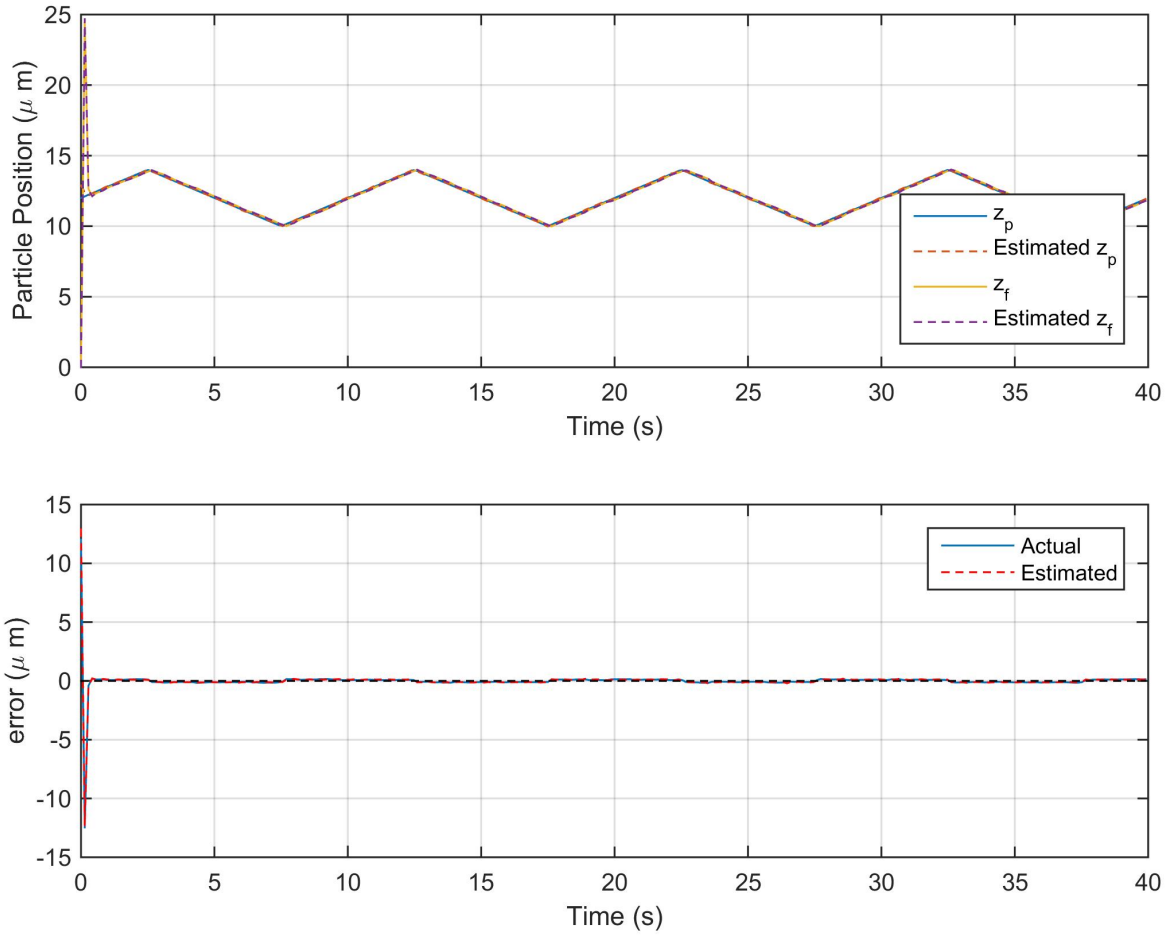

Figure 13

It can be seen in figure 13 that the system tracks the triangular wave. Looking more closely at the response, figure 14 shows that there exists a steady state error between the disturbance z_p and the response z_f which is approximately equal to 0.14 s. This is obvious as the settling time is 0.1 s and for a discrete time system, the response will show up in the next time step from the disturbance which is 0.14 s apart. So, this steady state error exists due to one-step delay between the disturbance and the response.

Figure 14 shows that the estimated values are a good approximation of the actual values. The difference between the two can be attributed to the measurement noise.

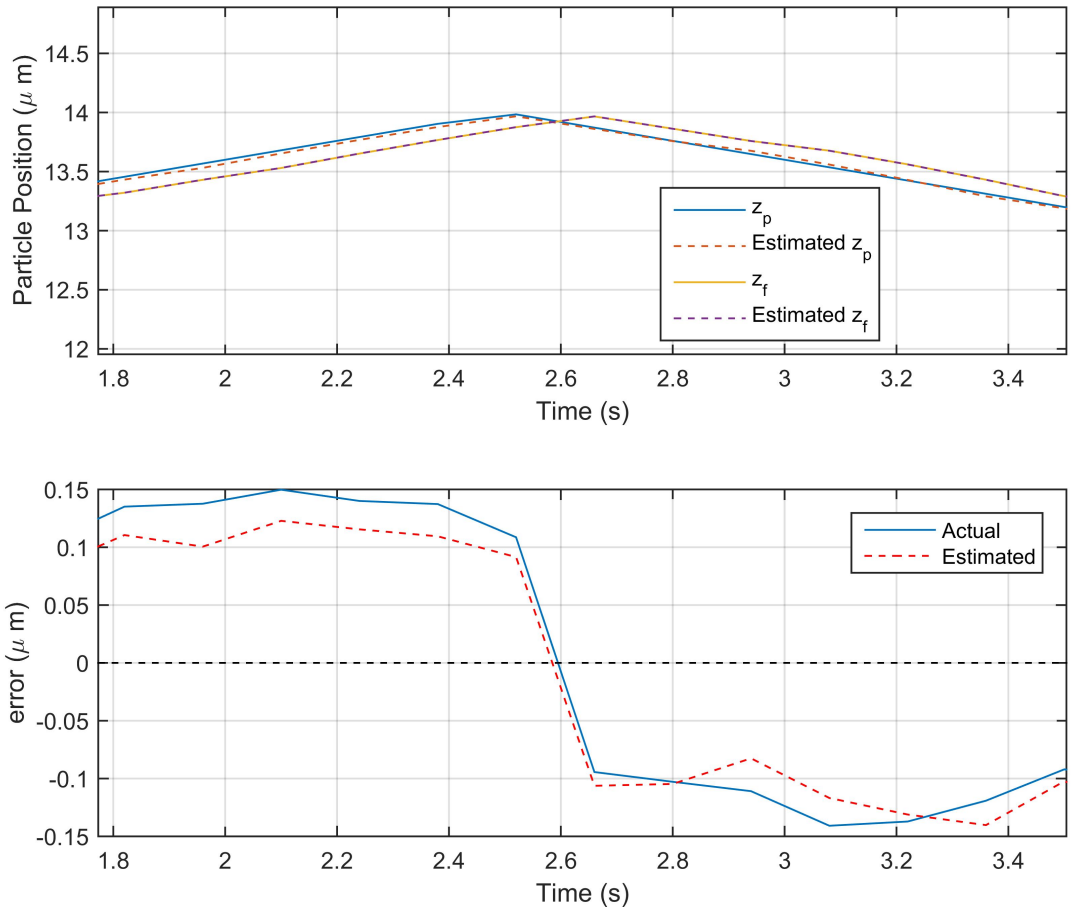

Figure 14: Figure 13 zoomed-in

Experiment

The digital control system is now implemented utilizing serial communication to devices, through a MATLAB code. Various z_{p0} values and a triangular disturbance in z_p are used to test the performance of the system. The disturbance is given from a different MATLAB session and the tracking control system is implemented through another independent MATLAB session. The results for $z_{p0} = 12\ \mu m.$, disturbance amplitude of $2\ \mu m$ and frequency of $0.1\ Hz$ are shown in figures 15 to 17.

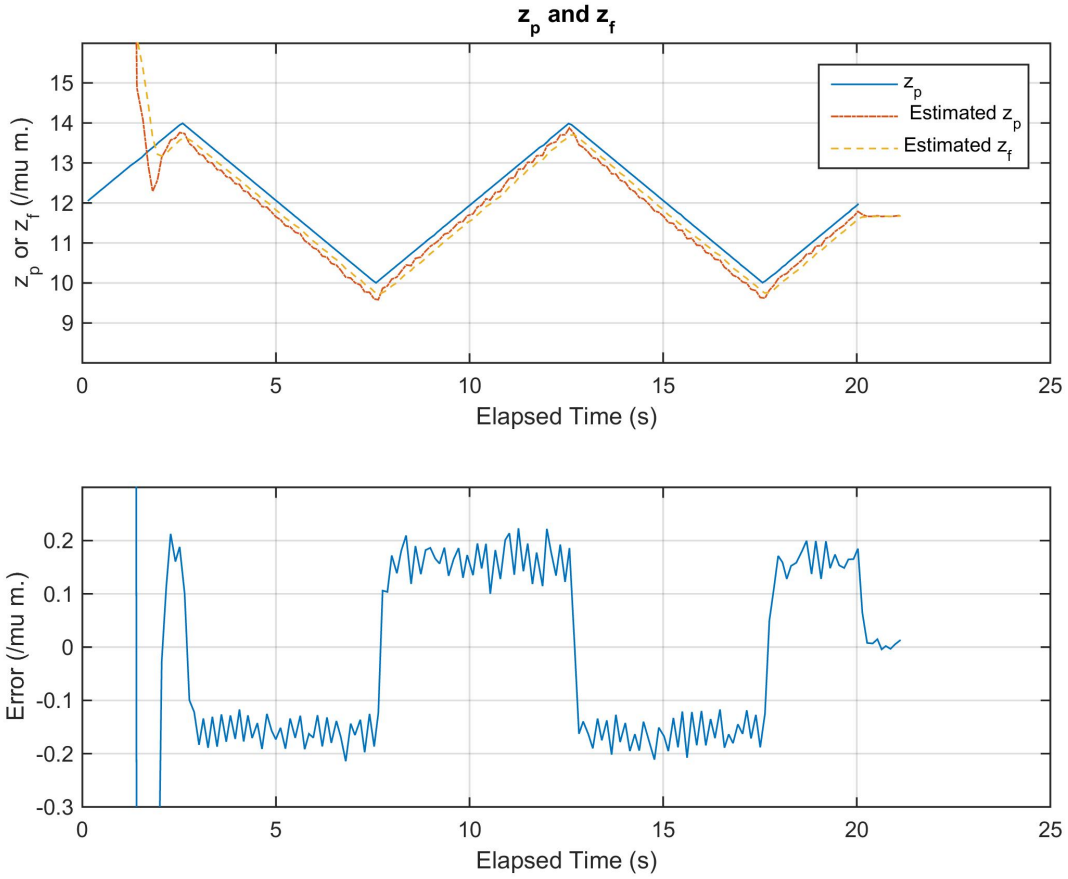

Figure 15

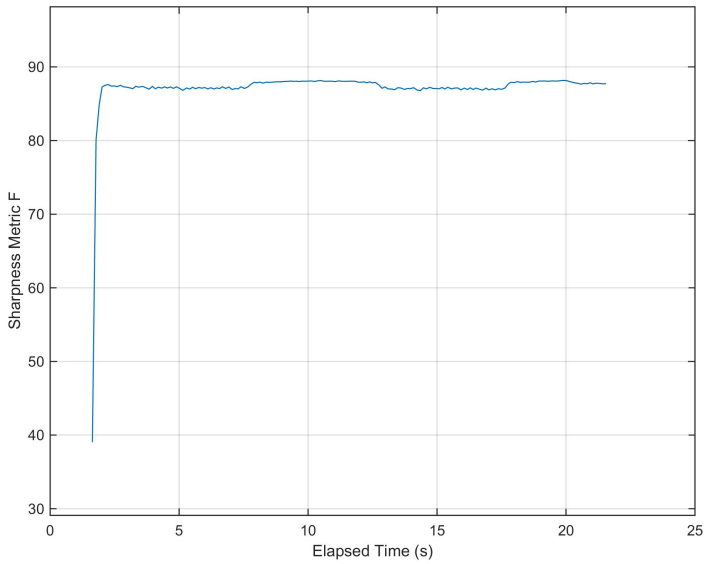

Figure 16

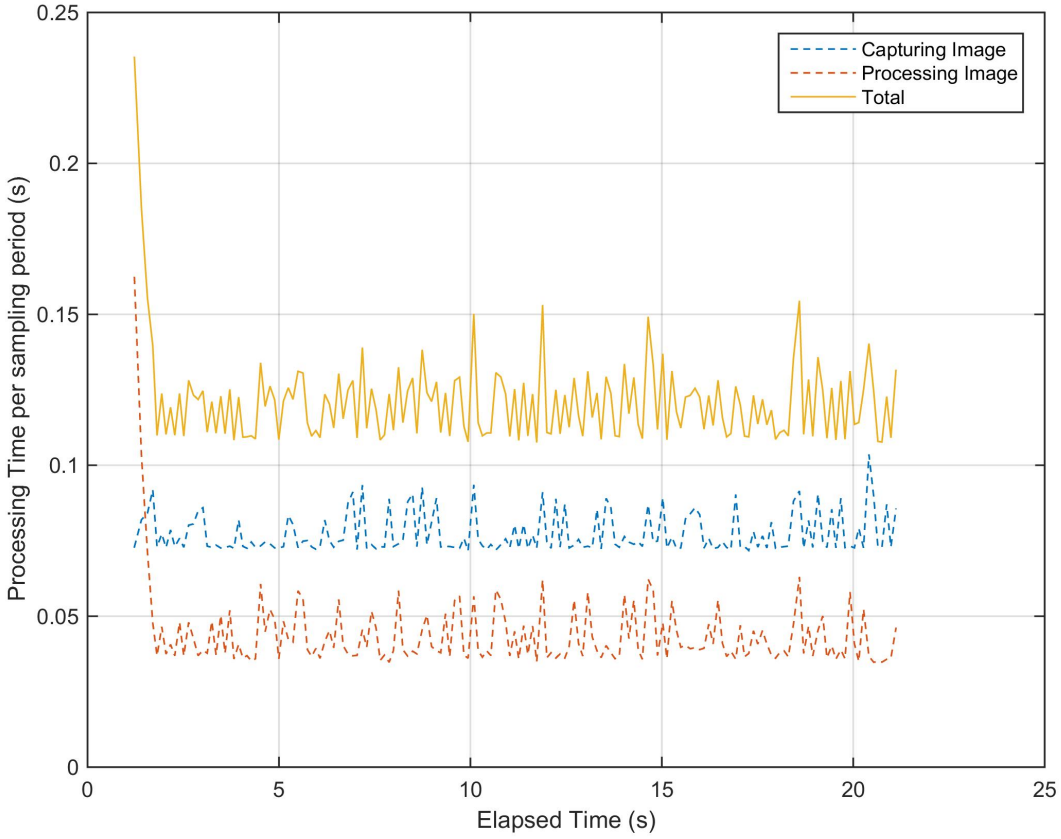

Figure 17: Computational times per sampling period

It can be seen from experimental results in figure 15 that $\hat{z}_p$ & $\hat{z}_f$ have the same relationship as seen in the simulation results but the z_p & $\hat{z}_p$ do not overlap each other as expected and there is a bias between the two. This bias may be due to the fact that during operation, the control current can heat up the lens, resulting in a temperature-dependent focus drift. Because the thermal focal-length expansion of a liquid lens is about two orders of magnitude larger than that of a glass lens, ETL's need integrated temperature sensors. The lens in use does have an integrated temperature sensor but it has not been utilized in this study as it would have introduced another parameter and made modeling of the system more complicated. However, these experimental results show that the temperature drift is very significant and it is essential to take the temperature changes into consideration while modeling this system.

Conclusion

This project successfully achieves its primary objective of designing a control system for an ETL enabling particle tracking in axial direction. The lack of direct state feedback data is dealt with using state estimation. The state, z_f, is estimated utilizing three pre-calibrated mathematical models and image processing. The models are not perfect but they enable the system to achieve its tracking objective satisfactorily. There are some discrepancies in the experimental results which can be attributed to the thermal focus drift of the liquid lens in use. Finally, it is concluded that thermal focus drift is significant and must be accounted while modeling the system for state estimation.

References

[1] Optotune, Datasheet: EL-16-40-TC, Electrically tunable large aperture lens, Update 24.05.2016, 2016

[2] Sun Y., Duthaler S., Nelson B.J., "Autofocusing Algorithm Selection in Computer Microscopy" *International Journal of Robotics Research*, Vol. 21, pp. 861-868, 2002.

[3] Gonzalez, R. C., R. E. Woods, and S. L. Eddins, *Digital Image Processing Using MATLAB*, First Edition, Pearson Prentice Hall, New Jersey, 2004.